Wear profiles and the dynamical simulation of wheel-rail systems

Martin Arnold* Helmuth Netter†,‡

Abstract

Recently, a quasi-elastic model for the contact between two rigid bodies was introduced, that is tailored to the contact between a wheel with wear profile and a rail ([1]). This new approach to the geometrical description of wheel-rail contact is used successfully in the dynamical simulation of wheel-rail systems that have wheels with wear profiles. In the present paper we discuss the application of the quasi-elastic contact model in the dynamical simulation and the efficient numerical solution of the model equations.

1 Introduction

Simulation tools get more and more important in the design and analysis process of modern advanced railway vehicle developments. Typical applications are parameter studies of the system behaviour in time or frequency domain to get an idea of the sensitivity of the design w. r. t. system parameters.

In this field the multibody system (MBS) approach is well established, i. e. the wheel-rail system is modelled as system of rigid or elastic bodies which are connected by massless joints, springs, dampers or active control elements. MBS models are composed of model components that are more or less self-contained. Among the model components that are specific for wheel-rail systems the most important one consists of conditions for the geometrical contact of wheel and rail and of a model for the friction forces between wheel and rail. Both problems are closely connected.

The traditional description of the wheel-rail contact in a MBS model is based on the geometry of two rigid bodies (wheel and rail) that touch in one single point,

*University of Rostock, Department of Mathematics, Postfach, D – 18051 Rostock, Germany, e-mail: arnold@mathematik.uni-rostock.d400.de

†Institute for Robotics and System Dynamics, DLR Oberpfaffenhofen, Postfach 1116, D – 82230 Wessling, Germany, e-mail: Helmuth.Netter@dlr.de

‡The work of both authors has been supported by the German Federal Minister for Education, Science, Research, and Technology (grant FR7ROK).

in the *contact point*. In real life, however, wheel and rail are elastically deformed in a neighbourhood of this contact point and there is a *contact patch* between wheel and rail. There are various models to compute the friction forces that act in this contact patch (see [3] for a comprehensive study of this subject).

From the numerical point of view a model for the contact of wheel and rail is attractive if

(M1) the condition for geometrical contact between wheel and rail is formulated as algebraic constraint (this avoids high-frequency oscillations in the solution that are typical of pure elastic models) and

(M2) the undeformed surfaces of wheel and rail are locally approximated by paraboloids so that a generalized Hertzian contact model can be applied (in this model the normal stress distribution in the contact patch is given in closed form using elliptic integrals).

If the assumptions (M1) and (M2) are satisfied then the motion of the wheel-rail system is described by the differential-algebraic system

$$\begin{aligned} M(q)\ddot{q} &= f(q,\dot{q},\lambda,t) - G^T(q)\lambda \\ 0 &= g(q) \end{aligned} \tag{1}$$

in the position coordinates $q(t)$ (see e. g. [7]). The Lagrangian multipliers $\lambda(t)$ couple the contact conditions $g(q) = 0$ with the dynamical equations. The constraint forces $-G^T(q)\lambda$ with $G(q) := \frac{\partial}{\partial q} g(q)$ guarantee that the constraints $g = 0$ are always satisfied. The vector $f(q,\dot{q},\lambda,t)$ consists of applied forces including the friction forces that depend on $-G^T(q)\lambda$. $M(q)$ denotes the (symmetric and positive definite) mass matrix.

The classical Hertzian contact model that has been used in various simulation packages results in efficient simulation tools for wheel-rail systems with conic wheels (that are frequently considered in theoretical investigations). However, it has been known since the early eighties (e. g. [4]) that this classical Hertzian contact model may result in large model errors if the wheels have a *wear profile*. These wheels are commonly used by European railway companies.

Recently, an alternative model for wheel-rail contact was proposed that considers the geometry of the (undeformed) surfaces of wheel and rail not only in the contact point but in the whole contact patch ([1]). This *quasi-elastic contact model* satisfies assumptions (M1) and (M2). It can be used both for systems with conic wheels and for systems having wheels with wear profiles. In the present paper we sketch the application of the quasi-elastic contact model in the industrial simulation package SIMPACK. In Section 2 we introduce basic notations and illustrate, why the classical approach fails for wear profiles. The quasi-elastic contact model is defined in Section 3. The numerical integration of the model equations (1) and simulation results for a benchmark of Pascal ([5]) are discussed in Section 4.

2 The geometry of wheel-rail contact

The basic unit of wheel-rail contact in the MBS model is the contact between one single wheel and a rail (Fig. 1). This allows the simulation both for wheel-rail systems with classical rigid wheelsets and for modern advanced railway vehicles without rigid coupling between the wheels of a wheelset. In local systems of coordinates $\boldsymbol{W}$ and $\boldsymbol{R}$ the undeformed surfaces of wheel and rail are given by industrial standards. The wheel is a body of revolution, its surface

$$\{ \, (\, F(s) \sin\tau \, , \, s \, , \, F(s) \cos\tau \,)^T \, : \, \tau \in [0, 2\pi), \, \underline{s} \le s \le \overline{s} \, \}$$

can be defined by a scalar *profile function* F that depends on the wheel coordinate s (in $\boldsymbol{W}$ the s-axis is parallel to the wheel axle). At the rail a system $\boldsymbol{R}$ of cartesian coordinates (u, v, w) is defined such that the u-axis is parallel to the track, the w-axis is oriented downwards and the origin of $\boldsymbol{W}$ lies in the (v, w)–plane (see Fig. 1). In general the rail profile may vary along the track (e. g. in switches), therefore the local geometry of the rail surface depends on the position x that the wheel has reached in its motion along the track. Locally, however, the changes of the profile in u-direction may be neglected and for a given position x the surface of the rail can be approximated by

$$\{ \, (\, u \, , \, v \, , \, G(v; x) \,)^T \, : \, u \in \mathbb{R}, \, \underline{v} \le v \le \overline{v} \, \}$$

with a profile function G that is independent of u. In special cases, e. g. in motions along a straight track with non-varying profile, the rail profile does not vary during the dynamical simulation, i. e. $G = G(v)$.

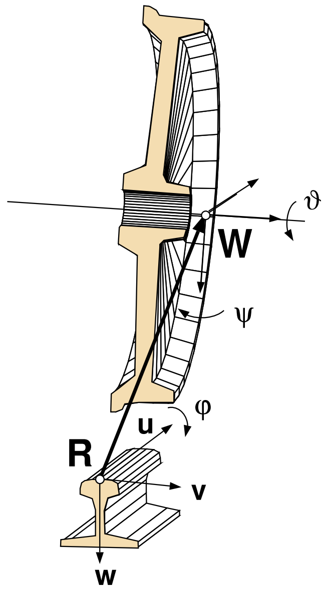

Figure 1: Geometry of wheel and rail.

As rigid body the wheel has 6 degrees of freedom and its relative position to the rail is determined by the coordinates (ξ_u, ξ_v, ξ_w) of the origin of $\boldsymbol{W}$ in $\boldsymbol{R}$ and by 3 angles of rotation $(\varphi, \vartheta, \psi)$ that are defined such that wheel axle, s-axis, and v-axis are parallel if $\varphi = \psi = 0$ ($\boldsymbol{R}$ was defined such that $\xi_u = 0$, see also Fig. 1). In $\boldsymbol{R}$ the wheel surface is given by

$$\{ \, (u, v, w)^T := (0, \xi_v, \xi_w)^T + A(\varphi, \psi) \cdot (F(s) \sin\tau, s, F(s) \cos\tau)^T \, \} \tag{2}$$

with a matrix $A(\varphi, \psi)$ that represents the rotations around the u- and the w-axis.

The contact condition determines the vertical displacement $\xi_w = \xi_w(\xi_v, \varphi, \psi; x)$ of the wheel as function of ξ_v, φ, and ψ. To be more specific we assign to each point P_{W} of the wheel surface a point $P_{\mathrm{r}}(P_{\mathrm{W}})$ of the rail surface by projection along the w-axis. For a classical contact point P_{W}^* the points P_{W}^* and $P_{\mathrm{r}}(P_{\mathrm{W}}^*)$ coincide and the normal vector $n_{\mathrm{W}}(P_{\mathrm{W}}^*)$ to the wheel surface at P_{W}^* is parallel to the normal

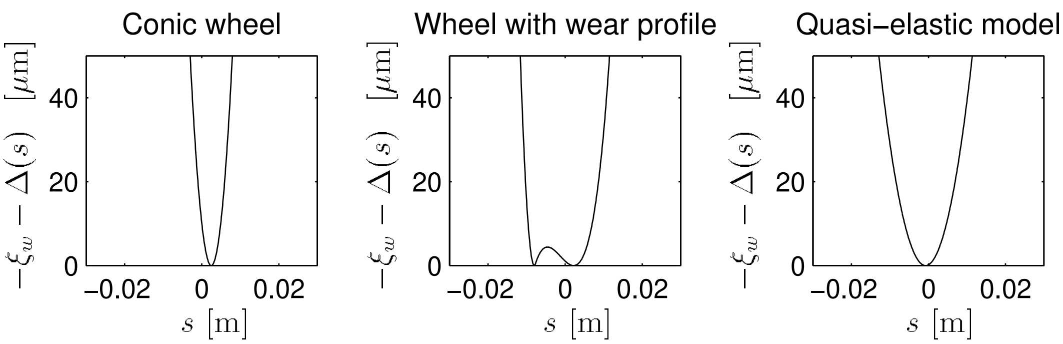

Figure 2: Distance between wheel and rail for points $P_{\mathrm{W}}(s;\psi) \in \mathfrak{C}$: Rail profile UIC60–ORE, $\xi_v = 9.67\,\mathrm{mm}$, $\varphi = 1.43°$, $\psi = 0°$. left plot: conic wheel, central plot: wheel profile S1002, right plot: distance between the paraboloids that approximate wheel (S1002) and rail in the generalized Hertzian contact model ($\nu = 2 \cdot 10^{-5}$).

vector $n_{\mathrm{r}}(P_{\mathrm{r}}(P_{\mathrm{W}}^*))$ to the rail surface at $P_{\mathrm{r}}(P_{\mathrm{W}}^*)$ (otherwise wheel and rail would penetrate each other).

With our assumptions all normal vectors n_{r} to the *rail* surface are parallel to the (v,w)–plane since G is independent of u. We define the curve $\mathfrak{C}$ as the curve of all points P_{W} on the *wheel* surface with normal vectors $n_{\mathrm{W}}(P_{\mathrm{W}})$ that are also parallel to the (v,w)–plane (i. e. $P_{\mathrm{W}}^* \in \mathfrak{C}$). In the special case $\psi = 0$ this curve $\mathfrak{C}$ consists of all points P_{W} that are directly below the centre of the wheel axle. In general $\mathfrak{C}$ depends on ψ and can be parametrized by the wheel coordinate s: $\mathfrak{C} = \mathfrak{C}(\psi) = \{\ P_{\mathrm{W}}(s;\psi)\ :\ \underline{s} \le s \le \overline{s}\ \}$. On $\mathfrak{C}$ we define the *height function*

$$\Delta(s;\xi_v,\varphi,\psi,x) := e_3^T \cdot (\ P_{\mathrm{W}}(s;\psi) - P_{\mathrm{r}}(P_{\mathrm{W}}(s;\psi))\ ) - \xi_w \tag{3}$$

that depends on ξ_v, φ, ψ, and x but is independent of ξ_w (see (2)).

The distance between $P_{\mathrm{W}}(s;\psi) \in \mathfrak{C}$ and $P_{\mathrm{r}}(P_{\mathrm{W}})$ is given by $\xi_w + \Delta(s;\xi_v,\varphi,\psi,x)$ (the distance is measured along the w-axis that is oriented downwards). Wheel and rail do not penetrate iff $\xi_w + \Delta(s;\xi_v,\varphi,\psi,x) \le 0$ is satisfied for all $P_{\mathrm{W}}(s;\psi) \in \mathfrak{C}$. Furthermore the undeformed bodies of wheel and rail are in contact iff

$$\xi_w + \max_s \Delta(s;\xi_v,\varphi,\psi,x) = 0\ . \tag{4}$$

In this classical contact model the contact point P_{W}^* is a point $P_{\mathrm{W}}^* = P_{\mathrm{W}}(s^*;\psi) \in \mathfrak{C}$ with $\Delta(s^*;\xi_v,\varphi,\psi,x) = \max_s \Delta(s;\xi_v,\varphi,\psi,x)$. Since the relative position of wheel and rail is determined by the MBS coordinates q this rigid body contact condition defines an algebraic constraint $g_i(q) = 0$. For a wheel-rail system with l wheels we get in (1) the constraint $0 = g(q) = (g_1(q),\ldots,g_l(q))^T$.

The critical point is the differentiability of g (g has to be at least two times continuously differentiable to get a continuous solution $q(t)$, $\lambda(t)$ of (1)). For conic wheels the height function has only one local maximum (Fig. 2 left) and the position s^* of the contact point varies smoothly with ξ_v, φ, and ψ. Therefore (4) defines in general a sufficiently differentiable constraint.

The central diagram of Fig. 2 shows the corresponding plot for a wheel with wear profile. These profiles are defined on the basis of measured data from wheels that are worn after frequent use. Therefore the surfaces of wheel and rail are approximately parallel over a large area of the tread. For the configuration in Fig. 2 (that is close to the nominal position of a wheel of a rigid wheelset on a straight track with rails inclined 1/40) there are two contact points. During the dynamical simulation jumps of the contact point occur and the constraint of the rigid body contact model is continuous, but only piecewise differentiable.

3 The quasi-elastic contact model

In [1] regularizations of the rigid body contact model (4) were discussed that use the information about the geometry of wheel and rail surface not only in one or more isolated point(s) but over the whole contact patch. Here we consider the *quasi-elastic contact model*

$$\xi_w + \mathrm{smax}_s^{(\nu)} \Delta(s; \xi_v, \varphi, \psi, x) = 0 \tag{5}$$

with

$$\mathrm{smax}_s^{(\nu)} \Delta(s; \xi_v, \varphi, \psi, x) := \nu \ln\Big(\int_{\mathfrak{C}} \exp(\frac{1}{\nu} \Delta(s; \xi_v, \varphi, \psi, x))\, ds \;/\; \int_{\mathfrak{C}} ds \Big) \tag{6}$$

and a small positive parameter ν. In the limit $\nu \to 0$ function $\mathrm{smax}_s^{(\nu)}\Delta$ converges (pointwise) to the maximum $\max_s \Delta$ but in contrast to (4) condition (5) defines for any $\nu > 0$ a sufficiently differentiable constraint (if Δ is sufficiently differentiable). In MBS coordinates the quasi-elastic contact condition (5) results in an algebraic constraint $g_i^{(\nu)}(q) = 0$, i. e. assumption (M1) of the Introduction is satisfied.

If $\nu > 0$ is small then the parts of $\mathfrak{C}$ that do not belong to the contact patch are negligible in $\int_{\mathfrak{C}} \exp(\frac{1}{\nu}\Delta)\, ds$ since $\exp(\frac{1}{\nu}\Delta)$ grows extremely fast if Δ is increased. We always have $\mathrm{smax}_s^{(\nu)} \Delta(s; \xi_v, \varphi, \psi, x) \leq \max_s \Delta(s; \xi_v, \varphi, \psi, x)$, i. e. (5) defines the vertical displacement ξ_w such that wheel and rail as rigid bodies would penetrate each other. The parameter ν in (6) is chosen so that $\max_s \Delta - \mathrm{smax}_s^{(\nu)} \Delta$ is of the same size as the elastic approach δ in a pure elastic model. (δ depends on the axle load, typical values are in the range of $10 \ldots 100\,\mu$m.) For profiles S1002 (wheel) and UIC60–ORE (rail) appropriate values of ν are in the range $10^{-5} \ldots 5 \cdot 10^{-5}$, in the actual computations we used $\nu = 2 \cdot 10^{-5}$. Then ξ_w in (5) is close to the vertical displacement of the wheel in a pure elastic contact model ("quasi-elastic" contact model).

In a rigid body contact model it is natural to suppose that constraint forces and friction forces act in the contact point P_{W}^*. The straightforward generalization to the quasi-elastic contact model considers constraint forces and friction forces that act in a point $P_{\mathrm{W}}(\tilde{s}; \psi) \in \mathfrak{C}$ where $\tilde{s}$ is defined as weighted mean value of s along $\mathfrak{C}$ with weights $\exp(\frac{1}{\nu}\Delta(s; \xi_v, \varphi, \psi, x))$:

$$\tilde{s} := \int_{\mathfrak{C}} s \cdot \exp(\frac{1}{\nu}\Delta(s;\xi_v,\varphi,\psi,x))\,ds \;/\; \int_{\mathfrak{C}} \exp(\frac{1}{\nu}\Delta(s;\xi_v,\varphi,\psi,x))\,ds\;. \qquad (7)$$

To get the friction forces we need an efficient method to compute the contact patch and the normal stress distribution in this contact patch (see (M2)). For conic wheels the classical Hertzian contact model can be used with paraboloids that approximate the surfaces of wheel and rail in a neighbourhood of the contact point. This is roughly illustrated by the left plot of Fig. 2 since the height function Δ coincides approximately with a parabola that has the contact point as apex. The central plot of Fig. 2 proves that the classical Hertzian contact model may result in large errors if the wheel has a wear profile. Here paraboloids with a contact point P_{W}^* as apex give only a very poor approximation of the surfaces of wheel and rail (see e. g. [4] for a more detailed discussion of non-Hertzian contact between a wheel with wear profile and a rail).

Eq. (7) motivates a generalization of the classical Hertzian contact model: the surfaces are approximated by paraboloids, but now with $P_{\mathrm{W}}(\tilde{s};\psi)$ as apex. The curvatures of the paraboloids are defined as weighted mean values of the curvatures of wheel surface and rail surface, respectively. Similar to (7) these mean values are computed along $\mathfrak{C}$ with weights $\exp(\frac{1}{\nu}\Delta)$. With this approach a reasonable approximation of the surfaces of wheel and rail in the contact patch is obtained. This is illustrated by the right plot of Fig. 2 that shows for the same configuration as in the central plot the height function if the surfaces of wheel and rail are substituted by these paraboloids ($\nu = 2 \cdot 10^{-5}$).

This generalized Hertzian contact model defines an *equivalent Hertzian contact patch* that can be obtained in the same way as in the classical Hertzian theory since assumption (M2) of the Introduction is satisfied. Software that has been developed originally for classical Hertzian contact patches (e. g. the code FASTSIM of Kalker [3]) can be carried over straightforwardly to compute the friction forces with an accuracy that is acceptable for most applications. Extensions to more complicated contact patches are currently under development.

4 The numerical solution of the model equations

To solve the model equations (1) efficiently the specific structure of the wheel-rail contact model in typical applications has to be exploited. Formulating the quasi-elastic contact model three essential points have been considered a priori: the assumptions (M1) and (M2) from the Introduction and the transition from the two dimensional surfaces of wheel and rail to the one dimensional curve $\mathfrak{C}$.

Eqs. (1) form a differential-algebraic system of index 3. Theory, numerical analysis and software for (1) are well developed (see [7] and the references therein). In the dynamical simulation the integral in (6) is discretized by the trapezoidal rule on a grid that is kept fixed during integration. With $\nu = 2 \cdot 10^{-5}$ the stepsize h_i

of the trapezoidal rule can be set to $h_i \approx 1\,\mathrm{mm}$ at the tread and $h_i \approx 0.2\,\mathrm{mm}$ at the flange of a wheel with wear profile S1002. Approximately 200 evaluations of Δ are necessary to compute one function value of $\mathrm{smax}_s^{(\nu)}$. The same discretization scheme is used to get the weighted mean values $\tilde{s}, \ldots$.

This basic implementation of the quasi-elastic model can be used in a wide range of applications including rail profiles that vary along the track (e. g. in switches) and wheelsets without rigid coupling of the wheels. The numerical effort to evaluate (5) is, however, much larger than in the classical rigid contact model (4).

In the simulation package SIMPACK this basic implementation is used only, if the rail profile really varies along the track, i. e. if G depends on x. However, in most of the industrial applications simulations have to be performed for non-varying rail profiles (straight tracks, curved tracks with fixed curvature). In this important special case the functions in (5) and (7) depend on ξ_v, φ, and ψ, only. They can be approximated by polynomial 3D–tensorproduct splines such that during the dynamical simulation the cpu-time for the evaluation of the contact condition is reduced drastically. Spline grid and spline order are adapted to the geometrical data of wheel-rail contact ([2]).

For given profile functions F and G the spline coefficients have to be computed only once, the splines can then be used in the simulation again and again. In SIMPACK the spline coefficients are computed during the model setup in a pre-processing step, i. e. before starting the simulation (for details see [2]). The spline approximation of the contact conditions reduces the overall simulation time by the factor $5 \ldots 12$, it is used as default whenever the rail profile does not vary along the track. We refer to [6] for the discussion of typical industrial applications of SIMPACK.

To illustrate the benefits of the quasi-elastic contact model and the importance of efficient numerical methods we end this section with simulation results for a model problem:

Example 1 Pascal ([5]) proposed as benchmark problem the motion of a rigid wheelset along a straight track with a force $F_y = 20\,\mathrm{kN}$ that acts in lateral direction and shifts the wheelset to the right. In (1) the wheelset is described by 6 position coordinates ($q(t) \in \mathbb{R}^6$) and 2 constraints (right/left wheel), the profile functions are S1002 (wheel) and UIC60 (rail). The motion tends to a quasi-stationary state ($y \approx 5.0\,\mathrm{mm}$) that is at the right wheel close to a configuration where the contact point P_{W}^* jumps. Fig. 3 shows that the rigid body contact model fails in this benchmark. The non-differentiability of (4) introduces discontinuities in $\lambda(t)$ and $\dot{q}(t)$ and artificial oscillations in $q(t)$. For the quasi-elastic contact model the quasi-stationary state is reached. The trajectory that is obtained using the basic implementation coincides with the one that is based on the (3D–)approximation of the geometrical data. The spline approximation reduces, however, the cpu-time for the dynamical simulation from 497.1 s to 42.4 s on a SUN Sparc5 workstation (i. e. by the factor 12).

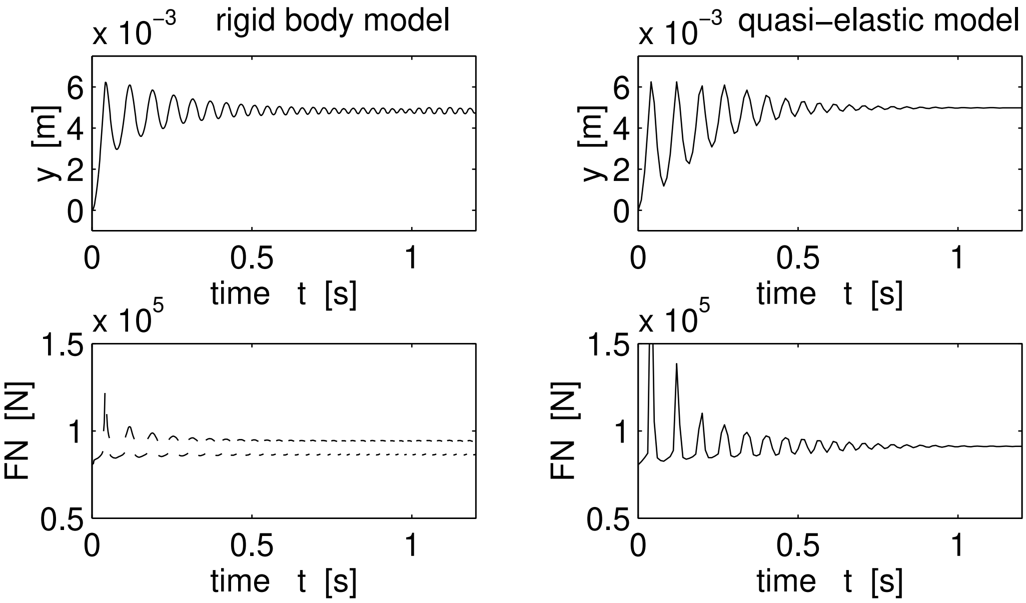

Figure 3: Rigid body contact model and quasi-elastic contact model applied to a benchmark of Pascal ([5]): lateral displacement y of the wheelset, constraint force FN at the right wheel.

References

[1] M. Arnold, K. Frischmuth, M. Hänler, and H. Netter. Differentialgleichungen und singuläre Mannigfaltigkeiten in der dynamischen Simulation von Rad–Schiene–Systemen. In K.-H. Hoffmann et al., editors, *Mathematik –Schlüsseltechnologie für die Zukunft*, Springer–Verlag, Berlin Heidelberg New York, (in press).

[2] M. Arnold and H. Netter. The approximation of contact conditions in the dynamical simulation of wheel-rail systems. Technical Report IB 515–96–08, German Aerospace Research Establishment, 1996.

[3] J.J. Kalker. *Three-Dimensional Elastic Bodies in Rolling Contact.* Kluwer Academic Publishers, Dordrecht Boston London, 1990.

[4] K. Knothe and H. Le The. A contribution to the calculation of the contact stress distribution between two elastic bodies of revolution with non-elliptic contact area. *Computers & Structures*, 18:1025–1033, 1984.

[5] J.P. Pascal. Benchmark to test wheel/rail contact forces. Technical report, INRETS Paris, 1990.

[6] W. Rulka, A. Haigermoser, L. Mauer, and H. Netter. Anwendung moderner Auslegungsstrategien für Schienenfahrzeuge durch Einsatz des Simulationsprogramms SIMPACK. VDI Berichte Nr. 1219, Düsseldorf, 1995.

[7] B. Simeon, C. Führer, and P. Rentrop. Differential-algebraic equations in vehicle system dynamics. *Surveys on Mathematics for Industry*, 1:1–37, 1991.